Solvation-Driven Excited-State Dynamics of [Re(4-Et-Pyridine)(CO)$_3$(2,2′-bipyridine)]$^+$ in Imidazolium Ionic Liquids. A Time-Resolved Infrared and Phosphorescence Study

Ana Maria Blanco-Rodríguez,[†] Kate L. Ronayne,[‡] Stanislav Záliš,[§] Jan Sýkora,[§] Martin Hof,[§] and Antonín Vlček, Jr.*[,†,§]

School of Biological and Chemical Sciences, Queen Mary, University of London, Mile End Road, London E1 4NS, United Kingdom, Central Laser Facility, Science and Technology Facilities Council, Rutherford Appleton Laboratory, Didcot, Oxfordshire OX11 0QX, United Kingdom, and J. Heyrovský Institute of Physical Chemistry, Academy of Sciences of the Czech Republic, Dolejškova 3, CZ-182 23 Prague, Czech Republic

Received: October 29, 2007; In Final Form: January 18, 2008

Excited-state dynamics of [Re(Etpy)(CO)$_3$(bpy)]$^+$ was studied in three imidazolium ionic liquids by time-resolved IR and emission spectroscopy on the picosecond to nanosecond time scale. Low-lying excited states were characterized by TD-DFT calculations, which also provided molecular dipole moment vectors in the relevant electronic states. TRIR spectra in ionic liquids show initial populations of two excited states: predominantly bpy-localized ^{3}IL and ^{3}MLCT, characterized by ν(CO) bands shifted to lower and higher frequencies, respectively, relative to the ground state. Internal conversion of ^{3}IL to the lowest triplet ^{3}MLCT occurred on a time scale commensurate with solvent relaxation. The ν(CO) IR bands of the ^{3}MLCT state undergo a dynamic shift to higher wavenumbers during relaxation. Its three-exponential kinetics were determined and attributed to vibrational cooling (units of picoseconds), energy dissipation to the bulk solvent (tens of picoseconds), and solvent relaxation, the lifetime of which increases with increasing viscosity: [EMIM]-BF_4 (330 ps) < [BMIM]BF_4 (470 ps) < [BMIM]PF_6 (1570 ps). Time-resolved phosphorescence spectra in [BMIM]PF_6 show a ∼2 ns drop in intensity due to the ^{3}IL → ^{3}MLCT conversion and a dynamic Stokes shift to lower energies with a lifetime decreasing from 1.8 ns at 21 °C to 1.1 ns at 37 °C, due to decreasing viscosity of the ionic liquid. It is proposed that solvent relaxation predominantly involves collective translational motions of ions. It drives the ^{3}IL → ^{3}MLCT conversion, increases charge reorganization in the lowest excited-state ^{3}MLCT, and affects vibrational anharmonic coupling, which together cause the dynamic shift of excited-state IR bands. TRIR spectroscopy of carbonyl−diimine complexes emerges as a new way to investigate various aspects of solvation dynamics, while the use of slowly relaxing ionic liquids offers new insight into the photophysics of Re(I) carbonyl polypyridyls.

Introduction

Solvent relaxation dynamics is usually studied by the time-dependent fluorescence Stokes shift of organic dyes, which serve as molecular solvation probes.[1−3] Electronic excitation of the dye molecule changes its electron density distribution and, hence, the magnitude and orientation of its dipole moment. The surrounding solvent molecules respond to the new charge distribution in the solute molecule. Reorientation of solvent dipoles or charges changes the electric field at the solute (so-called reaction field), stabilizing the excited state and destabilizing the ground state. This process is manifested experimentally as a dynamic red-shift of the fluorescence band whose kinetic analysis yields important information on solvent dynamics. This approach can be extended to more organized molecular media, such as proteins or membranes.[4,5] Surprisingly, there are almost no reports of solvent effects on excited-state dynamics of transition metal complexes, which are only very seldom used[6] as solvation probes.

Rhenium carbonyl−diimine complexes [Re(L)(CO)$_3$(α-diimine)]^n show a dynamic blue-shift of their stretching ν(C≡O) IR bands upon optical excitation into the Re → diimine metal-to-ligand charge-transfer (MLCT) excited state.[7−13] The strong medium dependence of the magnitude and kinetics of this IR shift suggests that time-resolved IR spectroscopy (TRIR) of organometallic carbonyl complexes can be employed as an alternative way of probing solvent relaxation dynamics. We have applied this approach to proteins (azurins) with appended Re(CO)$_3$(1,10-phenanthroline)$^+$ chromophores and demonstrated that the dynamic IR response to MLCT excitation depends on the character of the protein binding site to which the Re unit is attached.[9] Monitoring medium dynamics by excited-state IR spectra of transition metal carbonyl complexes is in many aspects different from the dynamic fluorescence shift of the usual organic relaxation probes. In principle, TRIR spectra could be sensitive to other modes of solute−solvent interactions than emission. They also could reflect vibrational cooling of the solute and heat transfer into the solvent bath. Indeed, studies in

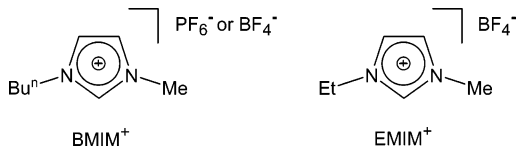

Figure 1. Imidazolium ionic liquids used in this study.

* Corresponding author. E-mail: a.vlcek@qmul.ac.uk.
† University of London.
‡ Rutherford Appleton Laboratory.
§ Academy of Sciences of the Czech Republic.

10.1021/jp710442v CCC: $40.75
Published on Web 03/29/2008

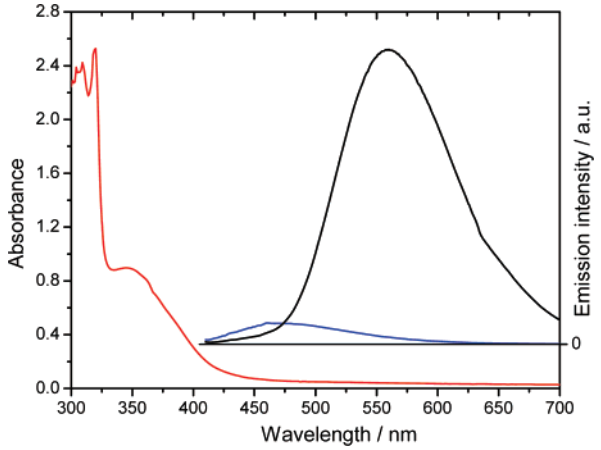

Figure 2. UV−vis absorption (red) and emission (black) spectra of [Re(Etpy)(CO)$_3$(bpy)]$^+$ in a [BMIM]PF$_6$ solution (Solvent Innovation GmbH) and neat [BMIM]PF$_6$ emission (blue). Excited at 405 nm. (See Figure S1 for spectra measured from Alfa-Aesar [BMIM]PF$_6$.)

CH_3CN and D_2O have shown[8−10,12,13] that relaxation monitored by TRIR extends into tens of picoseconds, which is much longer than observed using dynamic fluorescence Stokes shift with organic dyes.

Herein, we applied TRIR spectroscopy to study the relaxation dynamics of imidazolium-based ionic liquids (Figure 1). By using the complex [Re(Etpy)(CO)$_3$(bpy)]$^+$ as a probe, we were able to monitor the time evolution of both excited-state IR and phosphorescence spectra, which were found to report on the same type of solvation dynamics as the fluorescence Stokes shift of organic dyes.[3,14,15] Picosecond TRIR spectra also provided information on vibrational cooling, and, owing to slow relaxation in ionic liquids, provided the first direct evidence for the participation of both MLCT and intraligand triplet excited states in the photophysics of [Re(Etpy)(CO)$_3$(bpy)]$^+$.

Experimental Procedures

Materials. [Re(Etpy)(CO)$_3$(bpy)]PF$_6$ was prepared by a modified published procedure,[16] whereby [Re(OTf)(CO)$_3$(bpy)] was reacted with 4-ethylpyridine (Etpy) in THF. The product was characterized by IR and ^{1}H and ^{13}C NMR spectra. Ionic liquids were obtained from Alfa Aesar. [BMIM]PF$_6$ was purified[17] by washing with water and toluene, followed by treatment with active carbon and Al_2O_3 in acetone. Finally, it was degassed and dried in vacuum for 12 h at 80 °C. This treatment yielded [BMIM]PF$_6$, which shows only very weak luminescence, comparable to that described in the literature.[3,18] Time-resolved phosphorescence spectra also were measured with [BMIM]PF$_6$ purchased from Solvent Innovation GmbH, which was used as obtained. [Re(Etpy)(CO)$_3$(bpy)]PF$_6$ is well-soluble in imidazolium ionic liquids, although dissolving is rather slow. Undissolved solid can be removed by centrifuging.

Physical Measurements. Stationary UV−vis and FTIR absorption spectra were recorded using HP8453 and PE1720X spectrometers, respectively. Stationary emission spectra were obtained on the Jobin Yvon (Horiba) FluoroMax-3 and Fluorolog-3 instruments.

The TRIR experiments were carried out at the Central Laser Facility of the Rutherford Appleton Laboratory using an apparatus described in detail previously.[19−21] Briefly, part of the output from a 1 kHz, 800 nm, 150 fs, 1 mJ Ti-sapphire oscillator/regenerative amplifier (Spectra Physics Tsunami/Spitfire) was used to pump a white light continuum seeded β-barium borate (BBO) optical parametric amplifier (OPA). The signal and idler produced by this OPA were difference frequency mixed in a type I $AgGaS_2$ crystal to generate tunable broadband mid-infrared pulses (ca. 150 cm^{-1} fwhm and 0.1 μJ), which were split to give probe and reference pulses. The probe pulses were focused into the sample and imaged onto the input slit of a spectrograph (150 lines/mm). The reference pulses followed a similar optical path but were transmitted through air and then imaged into a second spectrograph. For experiments in the 1−2000 ps time range, second harmonic generation of the residual 800 nm light provided 400 nm pump pulses (∼150 fs fwhm and 3 μJ), which were sent along a delay line before exciting the sample at the magic angle. Both pump and probe pulses were focused to a diameter of 200−300 μm at the sample. Changes in infrared absorption at various pump−probe time delays were recorded by normalizing the outputs from a pair of 64-element HgCdTe (MCT) infrared linear array detectors on a shot-by-shot basis at 1 kHz. Data were collected in pump-on/pump-off pairs to minimize the effect of long-term drift in the laser intensity. The same equipment also was used in the nanosecond time domain. The sample was pumped by 355 nm, ∼0.7 ns fwhm, and ∼3 μJ laser pulses generated by an actively Q-switched AOT-YVO-20QSP/MOPA Nd:vanadate diode-pumped microlaser that was electronically synchronized with the femtosecond probe system.[21] The pump beam was set at the magic angle to the probe and focused to a diameter of 200−300 μm at the sample. The data were analyzed using Microcal Orgin 7.1 software. To determine the IR band maxima and widths, a sum of Gaussian functions was fitted to the experimental spectra measured at selected time delays.

Samples for TRIR measurements were prepared by dissolving [Re(Etpy)(CO)$_3$(bpy)]PF$_6$ in the ionic liquid (as obtained from Alfa Aesar) to give a solution with a ν(CO) IR absorbance of ca. 0.3. The solutions were placed in an IR transmission cell (Harrick Scientific Corp.) equipped with CaF_2 windows, one of which had a drilled circular groove ∼1 cm in diameter and 75 μm in depth to define the sample volume and path length. The cell was rapidly oscillated in the plane perpendicular to the direction of the laser beams to minimize laser heating and the potential build-up of decomposition products on the windows. The sample integrity was checked by FTIR spectra measured before and after each experiment.

Time-resolved emission spectra (TRES) were reconstructed from emission intensity decays measured by the time correlated single photon counting (TCSPC) technique on an IBH 5000 U instrument equipped with a cooled Hamamatsu R3809U-50 microchannel plate photomultiplier detector. The sample was excited at 405 nm with a diode laser (IBH NanoLED-07, fwhm 80 ps, and 500 kHz repetition rate). Separate measurements were performed in two time ranges, 0−2000 and 0−500 ns. Data were analyzed using the IBH Datastation2 software. The primary data consisted of a set of emission decays recorded at a series of wavelengths spanning the steady-state emission spectrum. TRES were calculated using the spectral reconstruction method.[1] The characteristics of the reconstructed TRES (e.g., fwhm and emission maxima) were obtained by a log-normal fitting.[1] Data analysis was complicated by background emission from [BMIM]-PF$_6$. Because of vastly different lifetimes of the emission from [BMIM]PF$_6$ (∼1.5 ± 0.1 and 7.8 ± 0.2 ns at 21 °C) and [Re(Etpy)(CO)$_3$(bpy)]$^+$ (218 ns), the [BMIM]PF$_6$ emission intensity is rather high at early times, even if its contribution to the stationary spectrum is negligible. In the spectral reconstruction procedure, the fast [BMIM]PF$_6$ emission decay can easily be projected onto the stationary spectrum of the Re complex, giving false results. To minimize this effect, we used higher concentra-

TABLE 1: Dynamic Shift Parameters[a] of A′(1) ν(CO) Band of $[Re(Etpy)(CO)_3(bpy)]^+$ in MeCN and Ionic Liquids Obtained at 21 °C

	CH_3CN	$[EMIM]BF_4$	$[BMIM]BF_4$	$[BMIM]PF_6$
		Fit to eq 1		
ν(GS)	2035.6	2033.7	2033.7	2034.6
$\nu(\infty)$	2075.7	2082.7	2076.1	2072.3
total shift	40.1	49	42.4	37.7
instantaneous shift	23.7	28.5	21.6	14.9
dynamic shift	16.4	20.5	20.8	22.8
A_f	11.8 ± 0.6	6.8 ± 0.6	4.5 ± 0.9	5.5 ± 0.8
A_m	4.6 ± 0.5	8.1 ± 1.5	7.2 ± 0.9	4.3 ± 0.6
A_s		5.6 ± 1.7	9.1 ± 0.9	13 ± 0.5
τ_f	1.0 ± 0.08	7.5 ± 1.2	6.8 ± 1.8	5.9 ± 1.8
τ_m	10.8 ± 1.0	78 ± 20	47 ± 14	82 ± 28
τ_s		334 ± 80	471 ± 69	1573 ± 109
		Fit to eq 2		
A_1		4.6 ± 1.06	1.7 ± 1.3[b]	5.6 ± 0.6
A_2		16.8 ± 1.5	20.8 ± 2.4[b]	16.8 ± 0.7
τ_1		6.5 ± 1.4	3.8 ± 3.4[b]	8.5 ± 1.8
β		0.63 ± 0.06	0.46 ± 0.06[b]	0.66 ± 0.05
τ_2		106 ± 16	135 ± 33[b]	1105 ± 82
$\langle\tau_2\rangle$		150	319	1485
		Solvent properties		
viscosity (η)	0.345	66.5	154	371
thermal diffusivity (κ)	10.7[c]	9.92[d]	10.29[d]	
			8.6[e]	7.5[e]
dielectric constant (ϵ_s)	35.9[f]	12.8[g]	11.7[g]	11.4[g]

[a] Band positions and pre-exponential factors A are quoted in cm^{-1}, and time constants τ are in ps. Solvent properties: η = viscosity[38−40] in cP, κ = thermal diffusivity in 10^{-8} m^2 s^{-1}, and ϵ_s = static dielectric constant.[10,41,42] The total and dynamic shifts are defined as $\nu(\infty) - \nu$(GS) and $A_f + A_m + A_s$, respectively. The instantaneous shift is the total minus the dynamic shift. $\langle\tau_2\rangle$ is the integral relaxation time calculated from the stretched-exponential term only: $(\tau_2/\beta)\Gamma(\beta^{-1})$ [b] Less accurate fit. [c] Ref 44. [d] Calculated from published values of heat capacity, thermal conductivity, and density; see http://ilthermo.boulder.nist.gov/ILThermo/mainmenu.uix. [e] Measured by transient grating.[43] [f] Ref 1. [g] Ref 41.

tions of $[Re(Etpy)(CO)_3(bpy)]^+$ in $[BMIM]PF_6$, giving an absorbance of 0.7 in a 1 cm cell. Time-resolved emission was then measured in two different ways. (i) Emission decay profiles at individual wavelengths were measured from neat $[BMIM]PF_6$ (Alfa-Aesar) and from the $[Re(Etpy)(CO)_3(bpy)]^+$ solution using the same acquisition time. The time-resolved emission spectra were then reconstructed from corrected decay profiles, which were obtained by subtracting the emission decays of $[BMIM]PF_6$ from those measured on the solution. The second set of measurements was performed using $[BMIM]PF_6$ from Solvent Innovation GmbH, which showed only very weak fluorescence upon excitation at 405 nm. The intensity of the $[BMIM]PF_6$ emission nearly disappeared upon the addition of $[Re(Etpy)(CO)_3(bpy)]^+$, presumably due to an internal filter effect of the Re complex at the excitation wavelength. Time-resolved emission spectra were then calculated directly from uncorrected decay curves. The good correspondence between the two types of measurement indicates that the interference of the $[BMIM]PF_6$ emission was minimized, if not removed. Compare Figure 2 (and Supporting Information Figure S1) and Figure 9 (and Supporting Information Figure S5) to see the results of both procedures.

DFT Calculations. The electronic structure of $[Re(Etpy)(CO)_3(bpy)]^+$ was calculated in vacuum by density functional theory (DFT) methods using the Gaussian 03[22] and Turbomole[23] program packages, employing the hybrid functional PBE0[24,25] (G03/PBE0). The structure of the lowest triplet excited-state a^3A'' was optimized by time-dependent DFT (TD−DFT) using Turbomole or by UKS calculations using G03. For H, C, N, and O atoms, either 6-31g* polarized double-ζ basis sets[26] or cc-pvdz correlation consistent polarized valence double-ζ basis sets[27] were used for geometry optimization and vibrational analysis and for the calculation of total density and electrostatic potential, respectively. Quasi-relativistic effective core pseudopotentials and a corresponding optimized set of basis functions for Re were employed in all programs.[28] The double-ζ SVP basis set was used for H, C, N, O, and halide atoms in Turbomole. The plots of the electrostatic potential were drawn using the GaussView program.

Results

UV−vis Absorption, Emission, and Ground-State FTIR Spectra. UV−vis absorption and emission spectra of $[Re(Etpy)(CO)_3(bpy)]^+$ are only weakly solvent-dependent. The lowest absorption band, due[16,29−31] to an allowed transition into the ^{1}MLCT-state b^1A', occurs in CH_3CN, acetone, and THF as a broad shoulder at ca. 340 nm, whereas a distinct band at 354 nm is seen in CH_2Cl_2. The emission band occurs at 551 nm in CH_2Cl_2 or $CHCl_3$, 561 nm in THF, and 566 nm in CH_3CN. An emission lifetime and quantum yield of ∼230 ns and 0.0287, respectively, were reported in degassed CH_3CN,[16] while a lifetime of 199 ± 0.2 ns was measured herein in air-saturated CH_3CN. The emission was attributed[16,29,30,32] to phosphorescence from the lowest triplet excited state, identified[29] by TD−DFT as the predominantly ^{3}MLCT-state a^3A''. A similar behavior was observed in $[BMIM]PF_6$ (Figure 2), where the lowest absorption and emission bands were found at ∼345 and 556 nm, respectively. The width (fwhm) measured in $[BMIM]PF_6$, 3480 cm^{-1}, was only slightly larger than in CH_3CN, 3370 cm^{-1}.

FTIR spectra of $[Re(Etpy)(CO)_3(bpy)]^+$ in all three ionic liquids show the highest ν(CO) band due to the in-phase A′(1) vibration at the same position as in CH_3CN, that is, at 2034 cm^{-1}; see lower panel of Figure 5 and Table 1. Uncharacteristically for a Re tricarbonyl complex with three nitrogen-coordinated ligands, the lower band due to the out-of-phase A′(2) and A″ vibrations shows two maxima at 1932 and 1922 cm^{-1} (see Figure 5). The shapes of the A′(1) bands in the ionic liquids and in CH_3CN are predominantly Gaussian and Lorentzian, respectively.

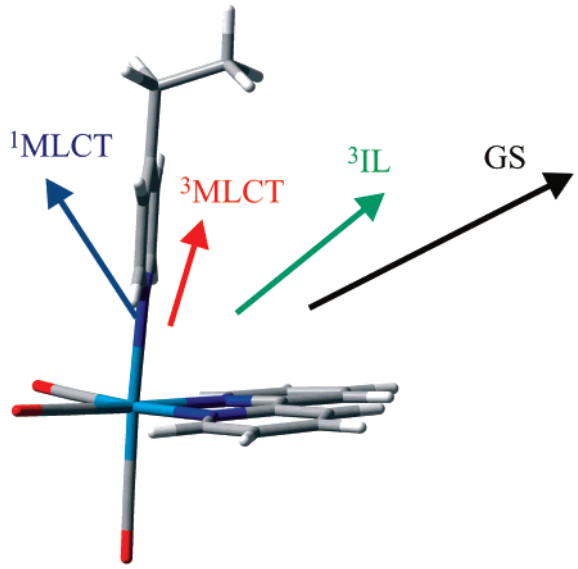

Figure 3. Relative size and orientation of dipole moment vectors of the ground-state (black) and excited-state ^{1}MLCT (b^{1}A′), ^{3}IL (b^{3}A″), and ^{3}MLCT (a^{3}A″) of [Re(Etpy)(CO)$_3$(bpy)]$^+$, projected onto the optimized ground-state molecular structure. Dipole moment vectors originate in the center of charge calculated using Mulliken population analysis. They lie in the molecular symmetry plane. (TD-DFT G03/PBE0/vacuum calculation at the optimized ground-state geometry.)

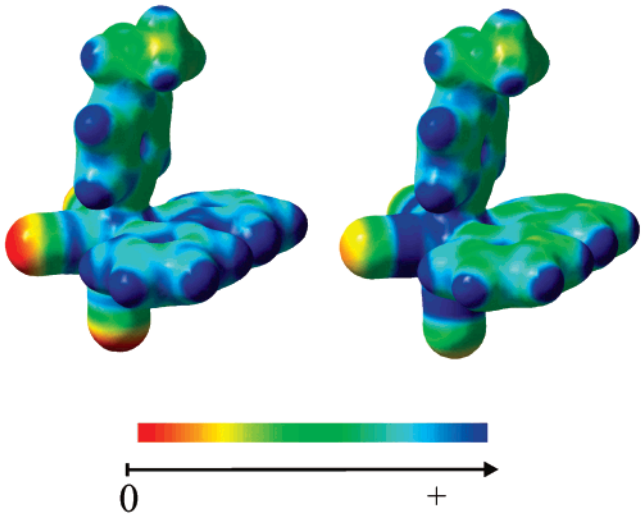

Figure 4. Mapping of the electrostatic potential onto an isodensity surface of the ground-state (left) and relaxed lowest triplet-state ^{3}MLCT (a^{3}A″) of [Re(4-Etpy)(CO)$_3$(bpy)]$^+$. (G03/PBE0 DFT calculation in vacuum.)

TD-DFT Excited-State Calculations. Low-lying singlet and triplet excited states and relevant Kohn−Sham orbitals are presented in Tables S1−S3, while Figure 3 shows dipole moments of states involved in the relaxation processes. The electrostatic potential around the molecule in its ground and lowest triplet excited state is depicted in Figure 4. The results were validated by a good correspondence of calculated and measured UV−vis transition energies (Table S1) and, for the lowest triplet state, with the excited-state IR spectrum.[30,32,33] Excited states are described by their predominant character, that is, MLCT or IL, as well as by a rigorous state notation where the prefix a, b, or c denotes the energy order of the excited states of a given spin multiplicity (1 or 3) and symmetry: A′ or A″. Thus, for example, a^{1}A′ is the ground state, b^{1}A′ is the first excited singlet state of the symmetry A′, and a^{3}A″ is the lowest triplet state of the symmetry A″, etc. The Kohn−Sham molecular orbitals reported in Table S3 were calculated without any symmetry constraints, but the aproximate symmetry within the C_s group is shown in parentheses. Orbitals are numbered consecutively in the order of increasing energy.

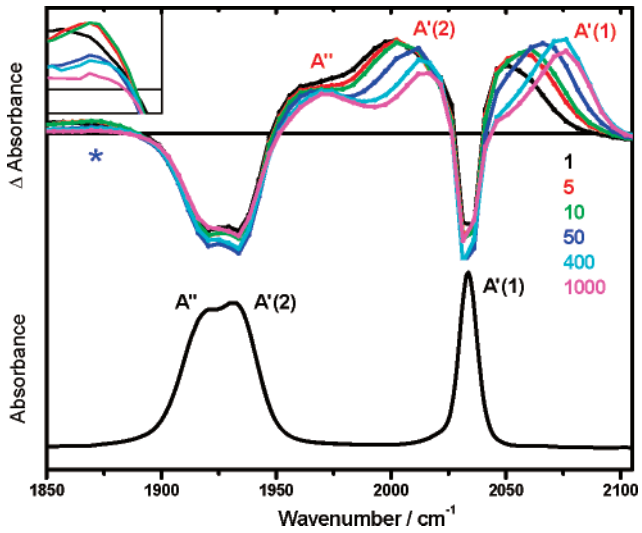

Figure 5. Difference time-resolved IR spectra of [Re(Etpy)(CO)$_3$(bpy)]$^+$ in [EMIM]BF$_4$ solution measured at selected time delays (ps) after excitation (top) and the corresponding ground-state FTIR spectrum (bottom). The inset shows magnification of the low-wavenumber region. The TRIR spectral resolution was 4.5−5.3 cm^{-1}. Bands of the ground state (black labels, bottom) and the ^{3}MLCT excited state (red labels, top) are assigned according to ref 30. The blue asterisk shows the low-energy band of ^{3}IL (b^{3}A″).

The lowest allowed electronic transition populates the b^{1}A′ state, which is predominantly Re(CO)$_3$ → bpy ^{1}MLCT. Optical excitation is accompanied by a decrease and reorientation of the molecular dipole moment and a shift of the center of charge (Figure 3), which are responsible for the negative solvatochromism of the lowest absorption band. Three low-lying triplet states were found to lie in a narrow energy range of about 0.5 eV. The third triplet b^{3}A″ is 79% intraligand (^{3}IL), originating in a $\pi \rightarrow \pi^*$ bpy-localized excitation, plus a 9% MLCT contribution. Hereinafter, it will be denoted as ^{3}IL. Accordingly, its dipole moment lies close to that of the ground state, with a slightly smaller magnitude. The lowest triplet-state a^{3}A″ is predominantly MLCT (86%), with a 9% IL contribution. Hereinafter, it will be known as ^{3}MLCT. Notably, this state is much less polar than the ground state, while the center of charge is strongly shifted toward the Re atom (Figures 3 and 4). The second triplet a^{3}A′ (MLCT) is not considered here since its population from b^{1}A′ or b^{3}A″ is symmetry forbidden.

TRIR Absorption Spectra. TRIR spectra of [Re(Etpy)(CO)$_3$(bpy)]$^+$ in ionic liquids were obtained at selected time delays after 400 nm and ∼150 fs laser pulse excitation. Figure 5 shows the spectra in [EMIM]PF$_6$ measured over the whole range of carbonyl stretching vibrations, ν(CO). The other two ionic liquids exhibit a very similar behavior (Figure S2). The images present the spectra measured at given times after excitation minus the spectrum measured without excitation (i.e., at a negative time delay). Positive spectral features thus correspond to the photogenerated excited state, and the negative peaks are due to depleted ground-state populations (bleach).

TRIR spectra measured at early times after excitation show a weak absorption feature at 1850−1880 cm^{-1} and three bands that occur at higher wavenumbers than the corresponding ground-state bands. The occurrence of the down-shifted 1850−1880 cm^{-1} absorption indicates[32] the population of a ^{3}IL state due to a $\pi \rightarrow \pi^*$ excitation of the bpy ligand, identified by

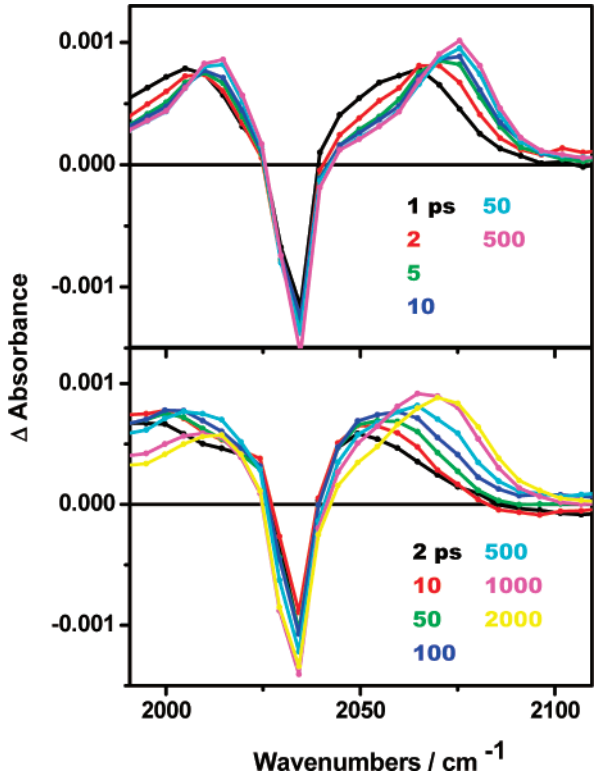

Figure 6. Dynamic evolution of the A′(2) and A′(1) excited-state IR bands of $[Re(Etpy)(CO)_3(bpy)]^+$ in CH_3CN (top) and $[BMIM]PF_6$ (bottom). TRIR spectra were measured at selected time delays (ps) after excitation. The spectral resolution was 4.5−5.3 cm^{-1}.

TD-DFT as b^3A''. The higher lying band expected[32] for ^{3}IL overlaps with other IR features, being manifested by the relatively large intensity of the middle band A′(2). The three upshifted bands are typical[8,20,30,32−37] of a ^{3}MLCT excited state. All the IR bands undergo a dynamic shift to higher wavenumbers, while the features due to ^{3}IL concomitantly decay in intensity (Figure 5), apparently due to conversion to ^{3}MLCT. The ^{3}IL features are clearly seen in $[EMIM]BF_4$ for at least 600−1000 ps and in $[BMIM]BF_4$ or $[BMIM]PF_6$ for 1−1.5 ns, but their lifetime cannot be evaluated quantitatively because of extensive band overlap, shift, and narrowing. The final ν(CO) TRIR spectral pattern seen at longer time delays represents[8,20,30,32−37] the relaxed lowest excited-state ^{3}MLCT (a^3A'').

The dynamic shift is most clearly observable on the relatively isolated highest A′(1) band of the ^{3}MLCT a^3A'' state (Figure 6). Its peak wavenumbers were determined by fitting the spectra to a sum of Gaussians (Figure S3) and then fitted to triexponential kinetics (eq 1). Alternatively, the expanded stretched-exponential kinetics (eq 2) also affords good fits. The results are summarized in Figure 7 and Table 1.

$$\tilde{\nu}(t) = \tilde{\nu}(\infty) - A_f \exp(-t/\tau_f) - A_m \exp(-t/\tau_m) - A_s \exp(-t/\tau_s) \quad (1)$$

$$\tilde{\nu}(t) = \tilde{\nu}(\infty) - A_1 \exp(-t/\tau_1) - A_2 \exp(-t/\tau_2)^{\beta} \quad (2)$$

Time-Resolved Phosphorescence Spectra. Phosphorescence of $[Re(Etpy)(CO)_3(bpy)]^+$ in air-saturated $[BMIM]PF_6$ decays with a lifetime of 218 ns, regardless of the emission wavelength. In addition, the decay curves contain one or two fast kinetic components observable during the first 10 ns, which are strongly dependent on the probe wavelength (Figure S4). Reconstructed

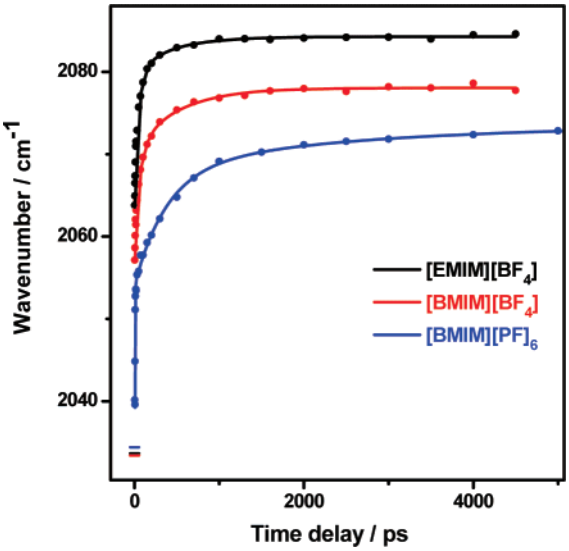

Figure 7. Time dependences of the peak wavenumbers of the excited-state A′(1) IR ν(CO) band of $[Re(Etpy)(CO)_3(bpy)]^+$ in ionic liquids. The curves are triexponential fits to eq 1. The horizontal lines at a zero time delay show the ground-state positions of the A′(1) band.

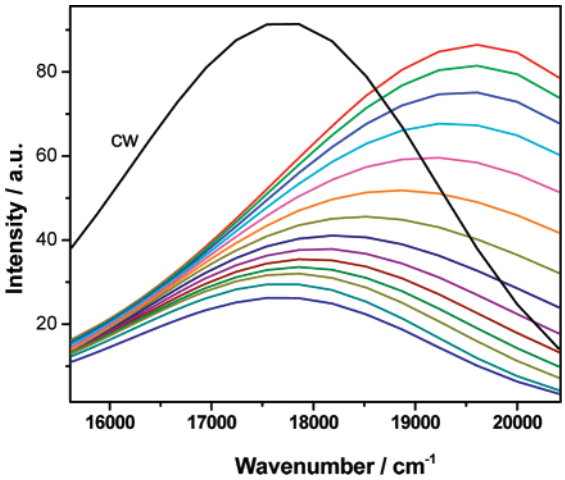

Figure 8. Reconstructed time-resolved phosphorescence spectra of $[Re(Etpy)(CO)_3(bpy)]^+$ in $[BMIM]PF_6$ at 21 °C at 0.24, 0.35, 0.5, 0.71, 1, 1.4, 2.1, 2.9, 4.2, 5.9, 8.5, 12.1, 24.6, and 50 ns, in the order of the red-shift and decreasing peak intensity. The cw curve is the stationary spectrum. Measured in $[BMIM]PF_6$ supplied by Solvent Innovations GmbH.

time-resolved spectra (Figure 8) show that the phosphorescence band of $[Re(Etpy)(CO)_3(bpy)]^+$ shifts to lower energies by 1900−2000 cm^{-1} during relaxation, with a principal lifetime of 1.8 ± 0.2 ns at 21 °C and 1.1 ± 0.1 ns at 37 °C (see Figure 9, top and Figure S5). The dynamic Stokes shift shows a minor (∼10%) long-lived component of about 10 ns, which we cannot determine accurately. Using a stretched-exponential does not improve the fit, giving only a small dispersion (β = 0.93 and τ = 1.9 ns). The dynamic Stokes shift is accompanied by changes in the bandwidth (Figure 9, bottom and Figure S5), which initially increases and then slowly decays over the next 15 ns. The fwhm reaches a maximum at 1.2 and 0.7 ns at 21 and 37 °C, respectively. The integrated area of the reconstructed phosphorescence band decays with a fast kinetic component of ca. 2.0 and 1.0 ns at 21 and 37 °C, respectively, plus the 218 ns excited-state lifetime (Figure S6). (In addition, there is a minor longer decay component, which cannot be determined accurately.)

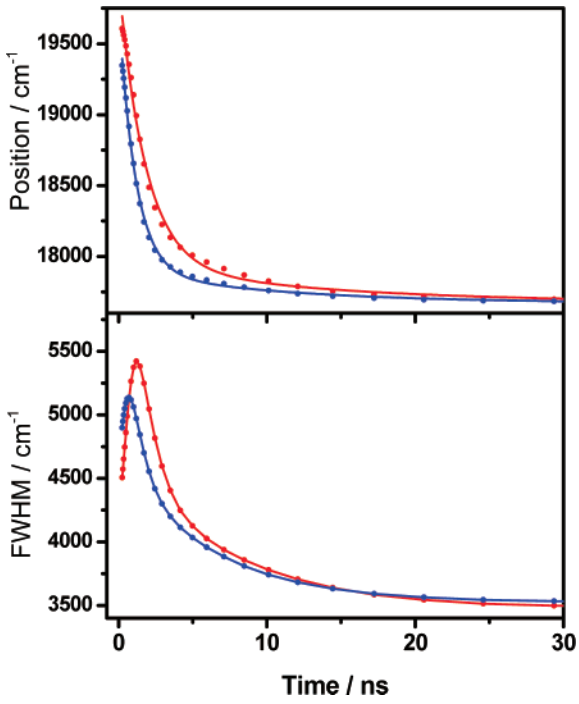

Figure 9. Time dependence of the peak position (top) and width (bottom) of the phosphorescence band of [Re(Etpy)(CO)$_3$(bpy)]$^+$ in [BMIM]PF$_6$. Red and blue data points were obtained at 21 and 37 °C, respectively. Measured in [BMIM]PF$_6$ supplied by Solvent Innovations GmbH.

Time-Resolved Phosphorescence Anisotropy. Decay of the emission anisotropy $r(t)$ of [Re(Etpy)(CO)$_3$(bpy)]$^+$ in [BMIM]-PF$_6$, measured at 560 and 600 nm over the range of 0.1−140 ns in steps 98 ps long, can be best fitted to a stretched-exponential with a wavelength-independent integral rotation time of 9.7 ns (fitted parameters: $\beta = 0.86 \pm 0.02$ and $\tau_r = 8.96 \pm 0.26$ ns at 560 nm and $\beta = 0.82 \pm 0.04$ and $\tau_r = 8.74 \pm 0.46$ ns at 600 nm). Single-exponential fits are also quite acceptable, affording rotation times of 10.1 ± 0.2 and 10.3 ± 0.3 ns at 560 and 600 nm, respectively. Observed rotation times are comparable to those reported for organic probes in [BMIM]PF$_6$.[45,46]

Discussion

Experimental results described above demonstrate the rich solvent-driven excited-state dynamics of [Re(Etpy)(CO)$_3$(bpy)]$^+$. The newly emerging picture of photophysics of Re carbonyl−diimine complexes, their use as IR probes of solvent relaxation dynamics, and implications for solvation in ionic liquids are based on the following observations, which will be discussed in detail: (i) the time-dependent change of the excited-state ν(CO) IR pattern, (ii) magnitudes and lifetimes of the dynamic shift of the excited-state ν(CO) A′(1) band, and (iii) the dynamic shift of the phosphorescence spectrum.

Electronic Excited States. Optical excitation of [Re(Etpy)-(CO)$_3$(bpy)]$^+$ at 400 nm prepares the ^{1}MLCT (b^{1}A′) excited state from which two triplet excited states, ^{3}IL (b^{3}A″) and ^{3}-MLCT (a^{3}A″), are populated simultaneously by ultrafast intersystem crossing (ISC) with a lifetime of 130 fs in CH$_3$-CN.[29] Since ISC is much faster than the time resolution of this study (∼1 ps), we attribute all the observed dynamics to the evolution and relaxation of the two triplet states ^{3}IL and ^{3}MLCT. The use of ionic liquids as solvents slows down relaxation processes and extends the lifetime of the upper ^{3}IL to such an extent that the population of both triplets is clearly manifested in the picosecond TRIR spectra by their distinct spectral patterns

SCHEME 1: Dynamic Behavior of the Position of the A′(1) ν(CO) Band after Excitation, as Described by Triexponential Kinetics (Eq 1)[a]

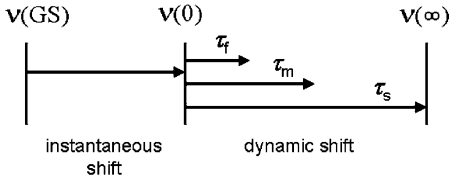

[a] Expanded stretched-exponential (eq 2) treats τ_m and τ_s as a single complex process.

(Figure 5). The relative population of the higher lying ^{3}IL state is rather small. It decays into the lowest triplet ^{3}MLCT by internal conversion with a rate commensurate with the slower stages of solvent relaxation: 1−2 ns in [BMIM]PF$_6$ and 870 fs[29] in CH$_3$CN.

Relaxation Processes in IR and Phosphorescence Spectra. The three IR bands of the lowest triplet-state ^{3}MLCT undergo a dynamic shift to higher wavenumbers, which is much slower in ionic liquids than in ordinary dipolar solvents or even proteins.[7−9] The magnitude and dynamics of the upward shift, measured for the A′(1) IR band, can be understood in terms of eq 1 and Scheme 1. Part of the shift, herein called instantaneous, occurs within the experimental time resolution (<1 ps). The dynamic shift follows with triexponential kinetics characterized by fast, middle, and slow lifetimes: τ_f, τ_m, and τ_s. The peak position of the excited-state A′(1) band ultimately converges to the value of $\nu(\infty)$, which corresponds to a fully relaxed a^{3}A″ MLCT state, thermally equilibrated both internally and externally (i.e., with respect to the medium). Extrapolation of $\nu(t)$ to $t = 0$ yields the value $\nu(0)$ that defines the instantaneous shift: $\nu(0) - \nu(\mathrm{GS})$.

The total IR shift, $\nu(\infty) - \nu(\mathrm{GS})$, reflects the extent of charge redistribution in [Re(Etpy)(CO)$_3$(bpy)]$^+$ on going from the electronic ground state to the relaxed ^{3}MLCT state. The detailed excited-state character and, hence, the total IR shift strongly depend on the medium. For example, total IR shifts of several Re complexes were found to decrease by at least 10 cm^{-1} on changing the solvent from CH$_3$CN to CH$_2$Cl$_2$, as the dielectric orientational response function decreases. Herein, it was found that the total shift decreases in the order [EMIM]BF$_4$ > [BMIM]-BF$_4$ > [BMIM]PF$_6$, which mostly is determined by the contribution from the instantaneous shift.

The instantaneous shift $\nu(0) - \nu(\mathrm{GS})$ reflects all the photophysical steps that are completed within the experimental time resolution of ca. 1 ps: optical excitation, electronic polarization of the solvent, ISC to the ^{3}MLCT state, and the inertial part of the solvent relaxation. The latter is known[15] to occur with a lifetime of 320−330 fs, and its contribution decreases as the combined size and reduced mass of the cation and anion of the liquid increases. Indeed, this is the order of decreasing magnitude of the instantaneous shift: [EMIM]BF$_4$ > [BMIM]BF$_4$ > [BMIM]PF$_6$. The absence of features attributable to $\nu = 1 \rightarrow 2$ hot ν(CO) vibrations in early TRIR spectra suggests that the energy released during the ISC is deposited on a subpicosecond time scale predominantly into low-frequency, large-amplitude intramolecular and solvent−solute vibrational modes of the lowest triplet state.

The processes responsible for the dynamic IR shift thus start from a hot ^{3}MLCT state that is excited in low-frequency vibrations, which are anharmonically coupled to the CO stretching modes. The fast kinetic component τ_f does not show any pronounced dependence on the ionic liquid (Table 1). Dynamic shifts of a comparable rate were measured[7,9,11] for

analogous Re complexes in alcohols, proteins, or at a ZrO_2 surface, while slightly faster rates were seen in CH_3CN or D_2O: 1.0−2.1 ps.[8−10,12,13] The observation of a very similar picosecond relaxation in various media allows us to attribute τ_f to vibrational cooling by energy dissipation into the immediate chromophore surroundings. High-frequency ν(CO) vibrations respond to cooling of low-frequency skeletal modes by a red-shift because of diminishing anharmonic coupling.

The middle kinetic component of the IR dynamic shift occurs in ionic liquids on a time scale of a few tens of picoseconds. A similar minor 11 ps component was observed in CH_3CN (Table 1), while values in the range of 9−20 ps were measured[8−10,12,13] for various cationic Re carbonyl−diimine complexes in CH_3CN or D_2O. Being much slower than the slowest relaxation time of CH_3CN (0.63 ps)[1], we propose[8] that the ∼11 ps dynamics in CH_3CN reflect slower stages of cooling, involving, namely, solute−solvent and first solvation sphere vibrations that are still anharmonically coupled to the ν(CO) vibrations. Cooling of the first solvation sphere vibrations amounts to heat diffusion from the immediate surroundings of the excited chromophore into the bulk solvent, and its rate should increase with increasing thermal diffusivity of the solvent.[47] The τ_m values measured in the ionic liquids do not correlate with any of their physical properties, and the middle relaxation is slower in ionic liquids than in CH_3CN despite only a small difference in thermal diffusivity (Table 1). Fluorescence studies using organic dyes have indicated[3] that the first stages of diffusive relaxation in ionic liquids occur with lifetimes of 130−280 ps. It is possible that the middle component of the IR dynamic shift in ionic liquids is a convolution of 10−20 ps solvent cooling and earlier stages of diffusive solvent relaxation. This conclusion is supported by the observation of 20−60 ps IR shift dynamics in alcohols, which were attributed to diffusive reorientation of solvent dipoles.[7,11] At the same time, the involvement of vibrational cooling of the excited solute and its closest environment in the fast and middle processes is corroborated by the accompanying sharp decrease of the A′(1) bandwidth.

The slow kinetic component τ_s increases with increasing viscosity of the ionic liquid in the order $[EMIM]BF_4$ (330 ps) < $[BMIM]BF_4$ (470 ps) < $[BMIM]PF_6$ (1570 ps), demonstrating that the underlying process involves structural reorganization of the solvent. An alternative fitting to the expanded stretched-exponential function (eq 2) assumes that the relaxation kinetics is composed of the fast component due to vibrational cooling (τ_1) and a complex nonexponential process, which is represented by the stretched-exponential term. In this interpretation, the medium and slow kinetics can no longer be attributed to physically distinct processes, and the integral relaxation lifetime $\langle\tau_2\rangle$ should be used to represent the solvent-dependent relaxation. Accordingly, $\langle\tau_2\rangle$ shows the same pronounced increase with increasing viscosity as τ_s (Table 1). The slow relaxation dynamics also clearly is manifested by the dynamic phosphorescence shift (Figures 8, 9, and S5), which occurs with a comparable lifetime: 1.8 ns at 21 °C. Acceleration of the phosphorescence shift to 1.1 ns on increasing the temperature to 37 °C is characteristic of ionic liquids, being caused by a decreasing viscosity.[45]

Solvent-Driven Excited-State Dynamics of $[Re(Etpy)(CO)_3(bpy)]^+$. The slow component of the IR shift dynamics (τ_s or $\langle\tau_2\rangle$), the phosphorescence shift, and the slower components of the dynamic fluorescence Stokes shift of organic dyes[3,14,15,45,48] all occur in ionic liquids with comparable lifetimes, which increase with increasing viscosity. All these experiments apparently report on the same aspects of the solvent response to the sudden charge redistribution in the excited solute molecule. The time-dependent emission maps the evolution of the energy of the emitting excited state along the solvent relaxation coordinate, while IR spectroscopy interrogates the changes of the intramolecular excited-state potential energy surface during solvent relaxation. The very fact that the CO stretching frequencies are affected by solvent relaxation demonstrates that evolutions along the intramolecular and solvation coordinates are to some extent coupled.

SCHEME 2: Solvation-Driven Excited-State Dynamics of $[Re(Etpy)(CO)_3(bpy)]^+$ in Ionic Liquids[a]

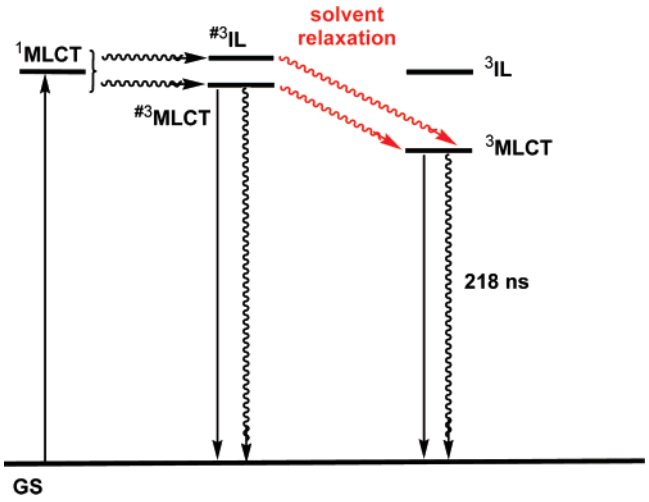

[a] # denotes a nonrelaxed (hot) state.

To understand the solvent-driven excited-state dynamics of $[Re(Etpy)(CO)_3(bpy)]^+$ (Scheme 2) and the mechanism whereby solvent relaxation affects excited-state ν(CO) vibrational frequencies, it is important to stress that the magnitude of the molecular dipole moment decreases upon MLCT excitation, while its vector changes direction and the charge center shifts toward Re (see Figure 3). In other words, the electric field gradient over the molecular surface is smaller in the ^{3}MLCT excited state than in the ground state, as is demonstrated in Figure 4. Immediately after excitation, the solvent is arranged around the $[Re(Etpy)(CO)_3(bpy)]^+$ solute molecules according to the ground-state charge distribution. The ^{3}MLCT state being less polar than the ground state, the initial arrangement of the solvent ions is more dense, organized, and oriented than is optimal for the new charge distribution in the excited state. The solvent thus initially exerts an electric field (reaction field) on the solute, which is oriented opposite to the charge redistribution due to electronic excitation. Interaction with this field increases the excited-state energy and restricts the charge redistribution. As the solvent relaxes, the electric field at the solute decreases. In consequence, the excited-state energy decreases, and the charge redistribution evolves to completion. This is manifested by shifting the phosphorescence and excited-state ν(CO) IR bands to lower and higher energies, respectively. The upper-state ^{3}IL is much less affected by the solvent relaxation because[49] its dipole moment is rather close to that of the ground state (Figure 3). The energy difference between the two triplet states therefore increases in the course of solvent relaxation, driving the ^{3}IL → ^{3}MLCT internal conversion. While the IR spectral patterns of the ^{3}IL and ^{3}MLCT states are distinct enough to be studied separately, the ^{3}IL and ^{3}MLCT phosphorescence largely overlap, giving rise to a single broad band.[29] The decay of the ^{3}IL population is manifested by the ca. 2 ns decay of the phosphorescence band area in $[BMIM]PF_6$ (assuming that the radiative rate constant is larger for ^{3}IL than ^{3}MLCT).

It is interesting to compare the mechanisms underlying the dynamic fluorescence Stokes shift of organic dyes and TRIR shifts of [Re(Etpy)(CO)$_3$(bpy)]$^+$. In both cases, the spectral changes result from the decrease of the excited-state energy as the reaction field adjusts to the excitation-induced charge redistribution in the solute. Organic dyes are usually regarded as nonpolarizable, and the dynamic spectral effects are attributed, in most general terms, to time-dependent solvation energy. The interpretation we propose herein for [Re(Etpy)(CO)$_3$(bpy)]$^+$ assumes that the solvation-driven change in excited-state energy drives intramolecular electronic changes, namely, the ^{3}IL → ^{3}MLCT conversion, and increases the charge redistribution in ^{3}MLCT. These effects can be viewed as time-dependent polarization of the excited Re complex by the reaction field.[50] A large polarizability of excited metal complexes results from their high excited-state density.

Finally, we should note that dynamic IR shifts also can arise from changes in anharmonic coupling caused by interactions between the time-dependent reaction field due to the solvent and the oscillating dipole of the solute vibration.[7] This outer-sphere mechanism probably presents only a smaller contribution to the spectral shifts seen for [Re(Etpy)(CO)$_3$(bpy)]$^+$. This conclusion is supported by the negligible solvent dependence of the ground-state IR spectra, by the rather large magnitude of the dynamic IR shift, and by pronounced relaxation effects on the intensities of excited-state UV absorption and resonance Raman bands.[8] Moreover, this mechanism can hardly explain the change in the IR spectral pattern and the decrease of emission intensity during relaxation.

Implications for Solvation and Electron-Transfer Dynamics in Ionic Liquids. Relaxation of ionic liquids consists of inertial and slower diffusive components.[15,48,51,52] The inertial part involves short-range correlated ion translations, each ion moving freely within its solvation cage.[15] Because of its shorter lifetime of about 300 fs,[15] inertial relaxation is not kinetically resolved in our experiments but contributes to the instantaneous shift. Several kinds of motion have been considered to occur on a slower time scale: large-scale restructuring of the solvent, reorientation of dipolar imidazolium cations, reorientation of dipolar ion pairs or clusters, and collective translational motions of ions.[3,15,39,41,46,48,51−58] Moreover, ionic liquids seem to be spatially heterogeneous on a time scale comparable to or longer than the solvation time,[3,18,40,59] containing nanometer-scale polar and nonpolar domains[60] and sets of ions with different diffusion rates.[61] Dynamic effects of specific $\pi-\pi$ solute−solvent interactions were observed for aromatic hydrocarbons in imidazolium ionic liquids.[59] Our TRIR and phosphorescence experiments generally agree with the view[14,15] that the slower part of ionic liquid relaxation consists predominantly of collective translational motions of ions, while the temporal evolution of the phosphorescence bandwidth (Figure 9) supports the suggestions of a spatial heterogeneity in [BMIM]PF$_6$.

Several studies have addressed electron-transfer (ET) reactivity in ionic liquids, in particular, the applicability of Marcus theory and the concept of outer-sphere reorganization energy, λ_o.[14,62−65] The observation of extensive solvent-driven dynamic spectral shifts demonstrates the importance of reorganization of the ionic liquid medium in response to charge transfer in the solute. Moreover, TRIR spectra indicate that solvent relaxation also contributes to internal reorganization. Values of λ_o pertinent to charge-transfer excitation of Coumarin 153 are comparable to those of high-polarity dipolar solvents.[14] They correlate with ion−ion separation or ion density in ionic liquids, instead of dielectric properties. Kinetics[63] and simulation[64,65] studies found λ_o values of ET reactions in ionic liquids similar to those in medium-polarity dipolar solvents, being dependent on the charge and electronic state of the solute[64,65] and on the solvation domain of spatially heterogeneous liquids. Slow solvation times imply a high degree of adiabaticity of ET reactions in ionic liquids. The rates of moderately exergonic ET reactions could be limited by the nanosecond rates of solvent reorganization, unless they occur[10] from hot excited states. On the other hand, highly exergonic ET reactions in ionic liquids may proceed with ultrafast rates into hot products,[66,67] followed by slower vibrational cooling and solvent relaxation.

Conclusion

Two triplet excited states of predominantly ^{3}IL or ^{3}MLCT character are populated within the first picosecond after optical excitation of [Re(Etpy)(CO)$_3$(bpy)]$^+$ in imidazolium ionic liquids.

Triplet excited states of [Re(Etpy)(CO)$_3$(bpy)]$^+$ undergo solvation-driven relaxation, which consists of ^{3}IL → ^{3}MLCT conversion, decrease of excited-state energy, and subtle changes of the excited-state character, namely, increasing the charge redistribution in the lowest ^{3}MLCT state. The dynamics of the excited-state relaxation reflects the dynamics of the solvent relaxation. Relaxation processes of [Re(Etpy)(CO)$_3$(bpy)]$^+$ are manifested in time-resolved IR and phosphorescence spectra by time-dependent band shifts, which thus report on various aspects of solvation dynamics.

[Re(Etpy)(CO)$_3$(bpy)]$^+$ and, presumably, other carbonyl−diimine complexes can be used as IR probes of solvation dynamics. The time dependence of their dynamic spectral shifts provides information on vibrational cooling, energy dissipation in the medium, and, importantly, slower kinetic components of solvent relaxation. Long intrinsic excited-state lifetimes enable the study of slow relaxation processes, which might not be accessible to organic fluorescent probes.

Vibrational cooling by energy transfer to the solvent is slower in ionic liquids, ∼7 ps, than in CH_3CN, ∼1 ps. Relaxation times of ionic liquids measured by TRIR spectra of [Re(Etpy)(CO)$_3$(bpy)]$^+$ were found to be 330, 470, and 1570 ps for [EMIM]BF$_4$, [BMIM]BF$_4$, and [BMIM]PF$_6$, respectively. They are very close to those obtained from dynamic phosphorescence shift (1.8 ns for [BMIM]PF$_6$) and to the slower part of dynamic fluorescence Stokes shifts measured[3,14,15] using organic dyes. Our results are consistent with the description[14,15] of ionic liquid relaxation as collective translational motions of ions and with a spatial heterogeneity in [BMIM]PF$_6$.

Acknowledgment. Funding by COST Action D35, The Science and Technology Facilities Council, Rutherford Appleton Laboratory (CMSD 43), QMUL, and the Ministry of Education of the Czech Republic (1P05OC68 and LC06063) is gratefully acknowledged. We thank Prof. M. Chergui (EPFL) for stimulating discussions.

Supporting Information Available: UV−vis and emission spectra, difference time-resolved IR spectra, Gaussian fits of TRIR spectra, emission decay curves, and time dependence graphics for [Re(Etpy)(CO)$_3$(bpy)]$^+$ and tables of transitions, energies, and compositions. This material is available free of charge via the Internet at http://pubs.acs.org.

References and Notes

(1) Horng, M. L.; Gardecki, J. A.; Papazyan, A.; Maroncelli, M. *J. Phys. Chem.* **1995**, *99*, 17311.

(2) Glasbeek, M.; Zhang, H. *Chem. Rev.* **2004**, *104*, 1929.
(3) Samanta, A. *J. Phys. Chem. B* **2006**, *110*, 13704.
(4) Pal, S. K.; Zewail, A. H. *Chem. Rev.* **2004**, *104*, 2099.
(5) Jurkiewicz, P.; Sýkora, J.; Olžinska, A.; Humpolíčková, J.; Hof, M. *J. Fluoresc.* **2005**, *15*, 883.
(6) Richert, R.; Stickel, F.; Fee, R. S.; Maroncelli, M. *Chem. Phys. Lett.* **1994**, *229*, 302.
(7) Asbury, J. B.; Wang, Y.; Lian, T. *Bull. Chem. Soc. Jpn.* **2002**, *75*, 973.
(8) Liard, D. J.; Busby, M.; Matousek, P.; Towrie, M.; Vlček, A., Jr. *J. Phys. Chem. A* **2004**, *108*, 2363.
(9) Blanco-Rodríguez, A. M.; Busby, M.; Grădinaru, C.; Crane, B. R.; Di Bilio, A. J.; Matousek, P.; Towrie, M.; Leigh, B. S.; Richards, J. H.; Vlček, A., Jr.; Gray, H. B. *J. Am. Chem. Soc.* **2006**, *128*, 4365.
(10) Liard, D. J.; Busby, M.; Farrell, I. R.; Matousek, P.; Towrie, M.; Vlček, A., Jr. *J. Phys. Chem. A* **2004**, *108*, 556.
(11) Lenchenkov, V. A.; She, C.; Lian, T. *J. Phys. Chem. B* **2004**, *108*, 16194.
(12) Busby, M.; Matousek, P.; Towrie, M.; Di Bilio, A. J.; Gray, H. B.; Vlček, A. *J. Inorg. Chem.* **2004**, *43*, 4994.
(13) Busby, M.; Matousek, P.; Towrie, M.; Clark, I. P.; Motevalli, M.; Hartl, F.; Vlček, A., Jr. *Inorg. Chem.* **2004**, *43*, 4523.
(14) Jin, H.; Baker, G. A.; Arzhantsev, S.; Dong, J.; Maroncelli, M. *J. Phys. Chem. B* **2007**, *111*, 7291.
(15) Arzhantsev, S.; Jin, H.; Baker, G. A.; Maroncelli, M. *J. Phys. Chem. B* **2007**, *111*, 4978.
(16) Hino, J. K.; Della Ciana, L.; Dressick, W. J.; Sullivan, B. P. *Inorg. Chem.* **1992**, *31*, 1072.
(17) Kavan, L.; Dunsch, L. *Chem. Phys. Chem.* **2003**, *4*, 944.
(18) Paul, A.; Mandal, P. K.; Samanta, A. *J. Phys. Chem. B* **2005**, *109*, 9148.
(19) Towrie, M.; Grills, D. C.; Dyer, J.; Weinstein, J. A.; Matousek, P.; Barton, R.; Bailey, P. D.; Subramaniam, N.; Kwok, W. M.; Ma, C. S.; Phillips, D.; Parker, A. W.; George, M. W. *Appl. Spectrosc.* **2003**, *57*, 367.
(20) Vlček, A., Jr.; Farrell, I. R.; Liard, D. J.; Matousek, P.; Towrie, M.; Parker, A. W.; Grills, D. C.; George, M. W. *J. Chem. Soc., Dalton Trans.* **2002**, 701.
(21) Towrie, M.; Parker, A. W.; Vlček, A., Jr.; Gabrielsson, A.; Blanco Rodriguez, A. M. *Appl. Spectrosc.* **2005**, *59*, 467.
(22) Frisch, M. J.; Trucks, G. W.; Schlegel, H. B.; Scuseria, G. E.; Robb, M. A.; Cheeseman, J. R.; Montgomery, J. A., Jr.; Vreven, T.; Kudin, K. N.; Burant, J. C.; Millam, J. M.; Iyengar, S. S.; Tomasi, J.; Barone, V.; Mennucci, B.; Cossi, M.; Scalmani, G.; Rega, N.; Petersson, G. A.; Nakatsuji, H.; Hada, M.; Ehara, M.; Toyota, K.; Fukuda, R.; Hasegawa, J.; Ishida, M.; Nakajima, T.; Honda, Y.; Kitao, O.; Nakai, H.; Klene, M.; Li, X.; Knox, J. E.; Hratchian, H. P.; Cross, J. B.; Bakken, V.; Adamo, C.; Jaramillo, J.; Gomperts, R.; Stratmann, R. E.; Yazyev, O.; Austin, A. J.; Cammi, R.; Pomelli, C.; Ochterski, J. W.; Ayala, P. Y.; Morokuma, K.; Voth, G. A.; Salvador, P.; Dannenberg, J. J.; Zakrzewski, V. G.; Dapprich, S.; Daniels, A. D.; Strain, M. C.; Farkas, O.; Malick, D. K.; Rabuck, A. D.; Raghavachari, K.; Foresman, J. B.; Ortiz, J. V.; Cui, Q.; Baboul, A. G.; Clifford, S.; Cioslowski, J.; Stefanov, B. B.; Liu, G.; Liashenko, A.; Piskorz, P.; Komaromi, I.; Martin, R. L.; Fox, D. J.; Keith, T.; Al-Laham, M. A.; Peng, C. Y.; Nanayakkara, A.; Challacombe, M.; Gill, P. M. W.; Johnson, B.; Chen, W.; Wong, M. W.; Gonzalez, C.; Pople, J. A. *Gaussian 03*, Revision C.02; Gaussian, Inc.: Pittsburgh, PA, 2004.
(23) Ahlrichs, R.; Bär, M.; Häser, M.; Horn, H.; Kölmel, C. *Chem. Phys. Lett.* **1989**, *162*, 165.
(24) Perdew, J. P.; Burke, K.; Ernzerhof, M. *Phys. Rev. Lett.* **1996**, *77*, 3865.
(25) Adamo, C.; Barone, V. *J. Chem. Phys.* **1999**, *110*, 6158.
(26) Hariharan, P. C.; Pople, J. A. *Theor. Chim. Acta* **1973**, *28*, 213.
(27) Woon, D. E.; Dunning, T. H., Jr. *J. Chem. Phys.* **1993**, *98*, 1358.
(28) Andrae, D.; Häussermann, U.; Dolg, M.; Stoll, H.; Preuss, H. *Theor. Chim. Acta* **1990**, *77*, 123.
(29) Cannizzo, A.; Blanco-Rodríguez, A. M.; Nahhas, A.; Šebera, J.; Záliš, S.; Vlček, A., Jr.; Chergui, M. *J. Am. Chem. Soc.* **2008**, *130*, in press.
(30) Dattelbaum, D. M.; Martin, R. L.; Schoonover, J. R.; Meyer, T. J. *J. Phys. Chem. A* **2004**, *108*, 3518.
(31) Martin, R. L. *J. Chem. Phys.* **2003**, *118*, 4775.
(32) Dattelbaum, D. M.; Omberg, K. M.; Hay, P. J.; Gebhart, N. L.; Martin, R. L.; Schoonover, J. R.; Meyer, T. J. *J. Phys. Chem. A* **2004**, *108*, 3527.
(33) Dattelbaum, D. M.; Omberg, K. M.; Schoonover, J. R.; Martin, R. L.; Meyer, T. J. *Inorg. Chem.* **2002**, *41*, 6071.
(34) Glyn, P.; George, M. W.; Hodges, P. M.; Turner, J. J. *J. Chem. Soc., Chem. Commun.* **1989**, 1655.
(35) George, M. W.; Johnson, F. P. A.; Westwell, J. R.; Hodges, P. M.; Turner, J. J. *J. Chem. Soc., Dalton Trans.* **1993**, 2977.
(36) Gamelin, D. R.; George, M. W.; Glyn, P.; Grevels, F.-W.; Johnson, F. P. A.; Klotzbücher, W.; Morrison, S. L.; Russell, G.; Schaffner, K.; Turner, J. J. *Inorg. Chem.* ***1994***, 33, 3246.
(37) Vlček, A., Jr.; Záliš, S. *Coord. Chem. Rev.* **2007**, *251*, 258.
(38) Seddon, K. R.; Stark, A.; Torres, M.-J. Viscosity and Density of 1-Alkyl-3-methylimidazolium Ionic Liquids. In *Clean Solvents: Alternative Media for Chemical Reactions and Processing*; Abraham, M., Moens, L., Eds.; American Chemical Society: Washington, DC, 2002; Vol. 819, p 34.
(39) Chowdhury, P. K.; Halder, M.; Sanders, L.; Calhoun, T.; Anderson, J. L.; Armstrong, D. W.; Song, X.; Petrich, J. W. *J. Phys. Chem. B* **2004**, *108*, 10245.
(40) Mandal, P. K.; Sarkar, M.; Samanta, A. *J. Phys. Chem. A* **2004**, *108*, 9048.
(41) Wakai, C.; Oleinikova, A.; Ott, M.; Weingärtner, H. *J. Phys. Chem. B* **2005**, *109*, 17028.
(42) Riddick, J. A.; Bunger, W. B.; Sakano, T. K. *Organic Solvents*; Wiley: New York, 1986.
(43) Frez, C.; Diebold, G. J.; Tran, C. D.; Yu, S. *J. Chem. Eng. Data* **2006**, *51*, 1250.
(44) Comeau, D.; Haché, A.; Melikechi, N. *Appl. Phys. Lett.* **2003**, *83*, 246.
(45) Ito, N.; Arzhantsev, S.; Maroncelli, M. *Chem. Phys. Lett.* **2004**, *396*, 83.
(46) Ingram, J. A.; Moog, R. S.; Ito, N.; Biswas, R.; Maroncelli, M. *J. Phys. Chem. B* **2003**, *107*, 5926.
(47) Iwata, K.; Hamaguchi, H. *J. Phys. Chem. A* **1997**, *101*, 632.
(48) Arzhantsev, S.; Jin, H.; Ito, N.; Maroncelli, M. *Chem. Phys. Lett.* **2006**, *417*, 524.
(49) Sensitivity of excited-state energy to dynamic solvation is proportional to the square of the dipole moment difference $(\vec{\mu}_e - \vec{\mu}_g)^2$, where the subscripts e and g denote the excited and ground state, respectively.[68]
(50) Increase of charge redistribution in the ^{3}MLCT (a^3A'') state during relaxation can be explained by decreasing its mixing with the upper ^{3}IL (b^3A'') state as their energy difference increases. The MLCT and IL characters of the a^3A'' and b^3A'' states thus become more pronounced, respectively.
(51) Kobrak, M. N.; Znamenskiy, V. *Chem. Phys. Lett.* **2004**, *395*, 127.
(52) Shim, Y.; Choi, M. Y.; Kim, H. J. *J. Chem. Phys.* **2005**, *122*, 44511.
(53) Lang, B.; Angulo, G.; Vauthey, E. *J. Phys. Chem. A* ***2006***, *110*, 7028.
(54) Headley, L. S.; Mukherjee, P.; Anderson, J. L.; Ding, R.; Halder, M.; Armstrong, D. W.; Song, X.; Petrich, J. W. *J. Phys. Chem. A* **2006**, *110*, 9549.
(55) Halder, M.; Headley, L. S.; Mukherjee, P.; Song, X.; Petrich, J. W. *J. Phys. Chem. A* **2006**, *110*, 8623.
(56) Daguenet, C.; Dyson, P. J.; Krossing, I.; Oleinikova, A.; Slattery, J.; Wakai, C.; Weingärtner, H. *J. Phys. Chem. B* **2006**, *110*, 12682.
(57) Znamenskiy, V.; Kobrak, M. N. *J. Phys. Chem. B* **2004**, *108*, 1072.
(58) Shim, Y.; Choi, M. Y.; Kim, H. J. *J. Chem. Phys.* **2005**, *122*, 44510.
(59) Iwata, K.; Kakita, M.; Hamaguchi-H. *J. Phys. Chem. B* **2007**, *111*, 4914.
(60) Canongia Lopes, J. N. A.; Pádua, A. A. H. *J. Phys. Chem. B* **2006**, *110*, 3330.
(61) Hu, Z.; Margulis, C. J. *Proc. Natl. Acad. Sci. U.S.A.* **2006**, *103*, 831.
(62) Grampp, G.; Kattnig, D.; Mladenova, B. *Spectrochim. Acta, Part A* **2006**, *63*, 821.
(63) Vieira, R. C.; Falvey, D. E. *J. Phys. Chem. B* **2007**, *111*, 5023.
(64) Lynden-Bell, R. M. *J. Phys. Chem. B* **2007**, *111*, 10800.
(65) Shim, Y.; Kim, H. J. *J. Phys. Chem. B* **2007**, *111*, 4510.
(66) Jortner, J.; Bixon, M. *J. Chem. Phys.* **1988**, *88*, 167.
(67) Gabrielsson, A.; Hartl, F.; Zhang, H.; Lindsay Smith, J. R.; Towrie, M.; Vlček, A., Jr.; Perutz, R. N. *J. Am. Chem. Soc.* **2006**, *128*, 4253.
(68) van der Zwan, G.; Hynes, J. T. *J. Phys. Chem.* **1985**, *89*, 4181.